A Wide-Band Microwave Photonic Phase and Frequency Shifter

S. T. Winnall, A. C. Lindsay, and G. A. Knight

***Abstract*— Advanced radar deception systems require wide-band devices which perform microwave processing of frequency and phase information. A wide-band microwave photonic phase shifter was constructed which is capable of imposing greater than 2π phase shift to microwave signals in the 2–18-GHz frequency range. The maximum standard deviation from the phase setting was 10° (7° typical). The phase shifter was then incorporated into a frequency translation architecture. The carrier suppression obtained was 50 dB with a spurious harmonic suppression of 23 dB.**

***Index Terms*—Integrated optics, microwave-frequency conversion, microwave phase shifters, optical-fiber devices, signal processing.**

I. Introduction

Many defense applications require the coverage of a large portion of the electromagnetic spectrum. There is significant interest in utilizing novel photonic architectures to perform signal processing functions in the microwave and millimeter-wave regime.

An example requirement of defense electronic countermeasures (ECM's) is the ability to perform velocity deception of Doppler radar. This involves using a frequency shift to impose a false Doppler signal on the returned radar pulse. A technique called serrodyning is often used to impose the frequency shift, where the microwave frequency is translated by the application of a linear phase ramp. Phase-shifting systems employing switched-line [1] or ferrite [2] technologies tend to have a narrow bandwidth of operation. Although monolithic microwave integrated circuit (MMIC) phase shifters have wide bandwidth of operation [3], the phase shift range is generally restricted, thus restricting their general utility.

A photonic phase shifter has been demonstrated and constructed, using the photonic analog of a technique known as vector modulation [4]. Previous systems have only reported operation at a single frequency [5], whereas the purpose of this paper is to investigate wide-band operation of the photonic phase shifter. A further aim was to use the photonic phase shifter as the basis for a serrodyne system to apply a controlled frequency shift to a microwave signal. The photonic architecture has the advantage of extremely wide-band operation when compared to traditional techniques, with potential for extension of the performance well into the millimeter-wave regime.

II. Phase Shifter

A. Phase Shifter Theory

The system to be analyzed is shown in Fig. 1. The input RF signal is split into in-phase and quadrature components by a 2–18-GHz 90° hybrid. The in-phase and quadrature signals are used to drive two 20-GHz Mach–Zehnder modulators labeled MZM#1 and MZM#2, respectively. The optical source for each modulator is a 1.3-μm semiconductor Fabry–Perot laser. The optical outputs from the modulators are then combined in an optical coupler and converted to an RF signal at the photodetector. Two separate lasers are used in order to prevent interference effects due to combining coherent laser modes at the coupler.

By appropriate choice of operating conditions, the photocurrent at the detector for RF frequency ω is given in Appendix I as

$$i_{\text{out}} = \frac{r}{4} P_o \alpha_m J_1(\Delta) \sin(\omega t + \phi + \beta_2) \tag{1}$$

where β_2 is a linear function of bias voltage V_2. The input signal is, therefore, shifted linearly in phase by varying the dc voltages V_2 and V_1, as originally shown in [5].

The photodetector current due to higher harmonics can be calculated by selecting appropriate terms of the Bessel function expansion of the modulator transfer function.

In practical systems, amplitude ripple of the hybrid and modulators gives rise to frequency-dependent phase ripple at the output signal. The equation for calculating frequency-dependent phase ripple is derived in Appendix I as

$$i_{\text{out}} = \frac{r}{4} P_o \alpha_m \sin(\omega t + \phi + \Psi(V, \omega)) \tag{2}$$

where

$$\Psi(V, \omega) = \arctan\left(\frac{J_1(\Delta_2)}{J_1(\Delta_1)} \tan \beta_2\right) \tag{3}$$

and the arguments are later defined in the Appendix.

For ideal modulator responses and zero hybrid ripple, the Bessel function ratio is unity and (2) is mathematically equivalent to (1), as required.

It can be shown from (3) that the rms phase noise due to laser intensity fluctuations is given by

$$\langle \Psi^2 \rangle = \frac{J_1^2(\Delta_1) J_1^2(\Delta_2)}{4} \sin^2(2\beta_2)(\text{RIN}_1 + \text{RIN}_2) \tag{4}$$

where RIN_1 and RIN_2 are the relative intensity noises of the lasers. Semiconductor diode lasers can have typically low RIN values (typically -140 dBc/Hz). The phase noise contribution will thus be much smaller than the phase variation which arises due to amplitude ripple associated with the hybrid and modulators.

B. Phase Shifter Experimental Procedure

The phase shifter was constructed as shown in Fig 1. The bias voltages at the photodetector were set to the values calculated from (A6). The laser powers were set to 2.5 mW giving a link insertion loss of approximately 60 dB. The output was then amplified by a wide-band amplifier with 45-dB gain over 2–18 GHz, resulting in a final RF insertion loss of 15 dB.

The fiber lengths were equalized with the coaxial line and the phase shift versus frequency was measured using the Wiltron 360B vector network analyzer. Fig. 2 illustrates the relative phase shift for bias settings corresponding to 40° phase increments. The maximum standard deviation from the phase setting corresponds to 10° (7° typical). Also shown in Fig. 2, is the theoretical model using (2), (3) and the S-parameter measurements of the hybrid and modulators (Appendix I).

The phase response compares well with wide-band state-of-the-art microwave phase-shift devices [3], [7].

Manuscript received December 18, 1995; revised February 28, 1997.

The authors are with the Electronics and Surveillance Research Laboratory, Salisbury, SA 5108 Australia.

Publisher Item Identifier S 0018-9480(97)03926-4.

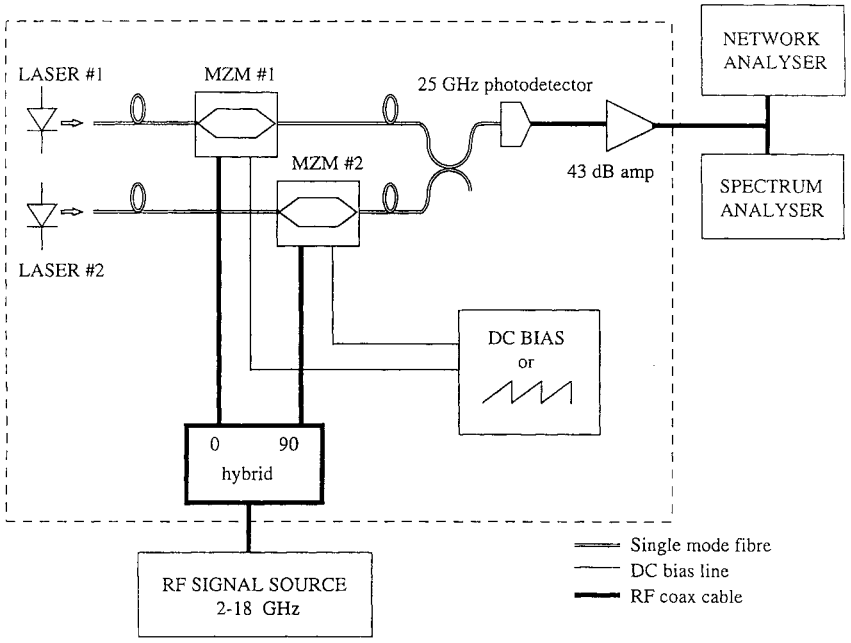

Fig. 1. Experimental layout of photonic phase shifter.

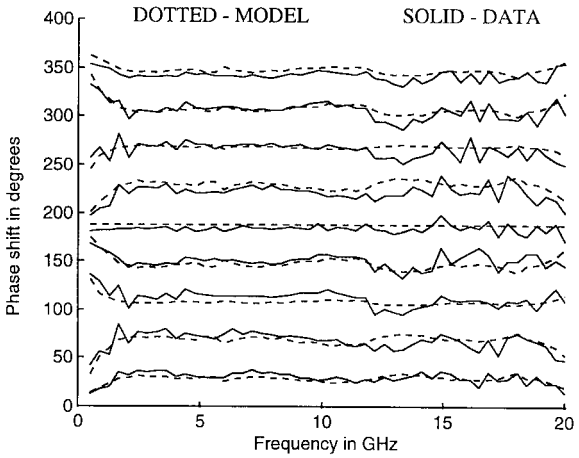

Fig. 2. Phase shift against frequency for 40° increments.

III. Frequency Translation System

General desirable features of false Doppler deception systems include a wide bandwidth of operation, the ability to suppress unwanted harmonics associated with the frequency translation process, and high suppression of the original carrier signal. It is expected that a photonic implementation should exhibit these features.

A. Serrodyne Theory

Phase shifters can be used as frequency translators for Doppler shifting a microwave carrier [1]. This technique is known as serrodyning. Serrodyne systems rely on the application of a linear phase ramp to shift the input carrier frequency. This phase function is implemented as a sawtooth function with amplitude 2π and period T. The voltage required to impose a particular Doppler shift is given by [6]

$$\frac{\Delta f}{f} = \frac{-2v}{c} \tag{5}$$

where

$$\Delta f = \frac{1}{2\pi}\frac{\partial \Phi}{\partial V}\frac{\partial V}{\partial t} \tag{6}$$

and

- Φ phase shift;
- V voltage required to impose this phase shift;
- f radar operating frequency;
- v false Doppler velocity.

For example, in order to impose a false velocity of 300 ms^{-1} on the return from a 10-GHz radar, a frequency shift of 20 kHz is required. Assuming modulators with a 5-V half-wave voltage, the phase ramp is required to reach 10 V in 50 μs. This is easily obtainable with commercial function generators. In conventional switched delay-line serrodyne systems [1], spurious harmonics are generated by the discrete nature of the phase ramp. With the system outlined in this paper, spurious harmonics are generated by the finite time to return from 2π to zero phase value. An ideal sawtooth function would produce a perfect tone. A computer model was developed to take into account the nonideal phase ramp. This involved simulating an RF signal at the required frequency, phase modulating the signal, and calculating the signal Fourier transform. The values obtained are consistent with the measured values of carrier and harmonic suppression.

B. Frequency Translator Experiment

Experimental Procedure: The experimental layout for the frequency translation experiment is shown in Fig. 1. The modulators were biased with a 20-kHz sawtooth voltage with a rise–fall time ratio of 18. Fig. 3 shows the frequency-shifted signal for an input frequency of 10 GHz. The harmonic suppression was 23 dB below the frequency-shifted signal and the carrier frequency was suppressed by 50 dB. The value harmonic suppression is typical of conventional serrodyne systems [1], but the carrier suppression of the photonic architecture is twice that of the system outlined in [1]. The levels of carrier and harmonic suppression can be improved by reducing the ramp fall-time value.

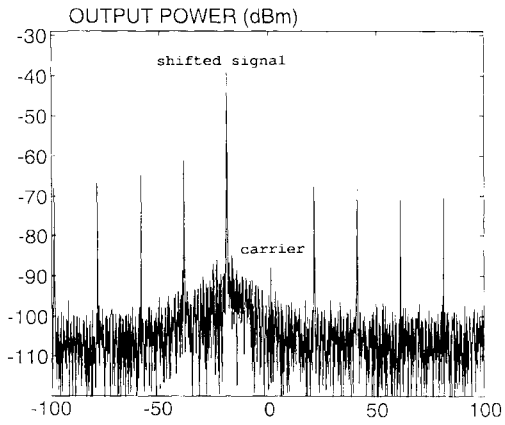

Fig. 3. Frequency-shifted spectrum for 10-GHz center frequency.

IV. Comparison with Microwave Devices

The photonic system has the advantage of wide bandwidth of operation. This is comparable to state-of-the-art MMIC devices [3], [7]. However, the photonic phase shifter has the capability to perform full 360° phase shifts. The ripple in the phase is of an equivalent performance. The bandwidth of operation can be increased by increasing the bandwidth of the hybrid and modulators.

The disadvantages of the photonic system include the high optical loss and cost of the fiber-optic link. Higher harmonics are also generated, as illustrated by the form of (A5). However, if the system application requires a photonic link, the photonic phase shifter allows a new degree of functionality to be incorporated.

V. Conclusion

A wide-band photonic phase shifter and frequency translator have been demonstrated. The phase shifter is capable of imposing a phase shift on a microwave signal of over 2π across the 2–18-GHz frequency range. This result compares favorably with MMIC phase-shifting techniques [3], [7].

The frequency shifter is capable of shifting a microwave carrier over the frequency range 2–18 GHz with a carrier suppression of 50 dB and a spurious harmonic suppression of 23 dB.

This system can be implemented as an optoelectronic integrated circuit (OIEC) in order to improve performance and reduce size and weight. Extension to cover the 4–40-GHz range is possible using existing technology.

Appendix

In this appendix, an expression for the photodetector current is obtained. The RF transfer function of the first Mach–Zehnder electro-optical modulator is given as

$$P_1 = \frac{P_1(0)\alpha_1}{2}\cos\left[\frac{\pi V_{m1}(\omega)}{V_{\pi 1}(\omega)}\sin(\omega t+\phi)+\frac{\pi V_1}{V_{\pi 1}(0)}+\psi_1\right]. \tag{A1}$$

Similarly, the output from MZM#2 (quadrature signal) is given by

$$P_2 = \frac{P_2(0)\alpha_2}{2}\cos\left[\frac{\pi V_{m2}(\omega)}{V_{\pi 2}(\omega)}\cos(\omega t+\phi)+\frac{\pi V_2}{V_{\pi 2}(0)}+\psi_2\right]. \tag{A2}$$

For convenience, assign the RF-dependent amplitudes as

$$\Delta_j = \frac{\pi V_{mj}(\omega)}{V_{\pi j}(\omega)}, \qquad j=1 \text{ or } 2 \tag{A3}$$

and the dc and static amplitudes as

$$\beta_j = \frac{\pi V_j}{V_{\pi j}(0)}+\psi_j, \qquad j=1 \text{ or } 2. \tag{A4}$$

The required signal component of the photocurrent at frequency ω is given by

$$i_{\text{out}} = \frac{r}{4}\big\{P_1\alpha_1 J_1(\Delta_1)\sin\beta_1\sin(\omega t+\phi) + P_2\alpha_2 J_1(\Delta_2)\sin\beta_2\cos(\omega t+\phi)\big\} \tag{A5}$$

where an extra factor of $\frac{1}{2}$ accounts for the 3-dB optical loss of the fiber coupler.

Initially the static bias setting for phase shift at dc needs to be determined. Applying the constraint $\sin\beta_1 = \cos\beta_2$ yields the condition

$$V_2 = \left[\frac{V_{\pi 2}(0)}{V_{\pi 1}(0)}\right]V_1 - \frac{V_{\pi 2}(0)}{2}+\frac{(\psi_2-\psi_1)V_{\pi 2}(0)}{\pi}. \tag{A6}$$

Equation (A6) is the relation between the bias voltages required to perform the phase shift. For two perfectly matched modulators $V_{\pi 1}=V_{\pi 2}=V_\pi$ and $\psi_1=\psi_2$. When this is the case, (A6) reduces to the expression $V_2 = V_1 - \frac{V_\pi}{2}$, similar to the expression found in [5]. With ideal modulators and correct adjustment of optical powers

$$i_{\text{out}} = \frac{r}{4}P_0\alpha_m J_1(\Delta)\sin(\omega t+\phi+\beta_2). \tag{A7}$$

Thus, the input signal is linearly shifted in phase by a dc voltage $V_2 = f(V_1)$.

For wide-band operation, differing modulator frequency responses give rise to a variation in the value of V_π [8]. Frequency-dependent amplitude ripple in the hybrid results in a varying input voltage at each modulator. Allow $\cos\Psi = J_1(\Delta_1)\sin\beta_1$ and $\sin\Psi = J_1(\Delta_2)\sin\beta_2$. By imposing the bias constraints $\sin\beta_1=\cos\beta_2$ and the optical power constraints $P_1\alpha_1 = P_2\alpha_2 = P_0\alpha_m$, (A7) now reduces to

$$i_{\text{out}} = \frac{r}{4}P_0\alpha_m\sin(\omega t+\phi+\Psi(V,\omega)) \tag{A8}$$

where

$$\Psi(V,\omega) = \arctan\left(\frac{J_1(\Delta_2)}{J_1(\Delta_1)}\tan\beta_2\right). \tag{A9}$$

The phase ripple with frequency needs to be estimated in terms of measured hybrid and modulator S-parameters. The available RF drive voltage is modeled as

$$V_1(\omega) = (P_{\text{in}}R_1)^{1/2}\left|S_{21}^{(I)}(\omega)\right|\sqrt{1-\left|S_{11}^{(1)}(\omega)\right|^2} \tag{A10}$$

where

- $S_{21}^{(I)}(\omega)$ the frequency-dependent transmission of the modulator;
- $S_{21}^{(1)}(\omega)$ the hybrid frequency-dependent ripple of the in-phase arm;
- $S_{11}^{(1)}(\omega)$ the input reflection coefficient of the modulator;
- P_{in} RF input power to the hybrid;
- R_1 terminating resistances of each modulator.

A similar expression exists for $V_2(\omega)$.

The frequency-dependent RF half-wave voltage is [8]

$$V_{\pi 1}(\omega) = V_{\pi 1}(0)10^{-|S_{21}^{(1)}(\omega)|/20}. \tag{A11}$$

Thus, the expression for the first argument of the Bessel function in (A5) is

$$\Delta_1 = \frac{\pi(P_{\text{in}}R_1)^{1/2}|S_{21}^{(I)}(\omega)|\sqrt{1-|S_{11}^{(1)}(\omega)|^2}}{V_{\pi 1}(0)10^{-|S_{21}^{(1)}(\omega)|/20}}. \tag{A12}$$

A similar expression exists for the argument of the second Bessel function.

REFERENCES

[1] A. Hodisan, "Digital phase shifters serve as frequency translators," *Microwaves RF*, pp. 61–72, July 1993.

[2] D. A. Charlton, "A low-cost construction technique for garnet and lithium-ferrite phase shifters," *IEEE Trans. Microwave Theory Tech.*, vol. 22, June 1974.

[3] S. Lucyszyn and I. D. Robertson, "Two-octave bandwidth monolithic analog phase shifter," *IEEE Microwave Guided Wave Lett.*, vol. 2, pp. 343–345, Aug. 1992.

[4] D. J. Ciardullo, "A high-accuracy phase shifter based on a vector modulator," *RF Design*, pp. 106–112, Oct. 1993.

[5] J. F. Coward, T. K. Yee, C. H. Chalfant, and P. H. Chang, "A photonic integrated-optic RF phase shifter for phased-array beamforming applications," *J. Lightwave Technol.*, vol. 11, Dec. 1993.

[6] M. I. Skolnik, *Introduction to Radar Systems*. New York: McGraw-Hill, 1980, p. 69.

[7] G. St. Onge, C. Wutke, C. Barratt, W. Coughlin, and J. Chickanosky, "A fully monolithic 4–18-GHz digital vector modulator," *IEEE MTT-S Dig.*, pp. 789–792, 1990.

[8] G. K. Gopalakrishnan, W. K. Burns, R. W. McElhanon, C. H. Bulmer, and A. S. Greenblat, "Performance and modeling of broadband $LiNbO_3$ travelling wave optical intensity modulators" *J. Lightwave Technol.*, vol. 12, no. 10, pp. 1807–1818, Oct. 1994.